
Araştırma Makalesi / Research Article

Examination of $^{11}\text{Be}+d$ Reaction with Different Nuclear Potentials

Murat AYGÜN^{1*}

¹ Bitlis Eren University, Department of Physics, Bitlis, 13000, Turkey

Abstract

In this study, we aim to see the efficiency of various nuclear potentials in explaining the elastic scattering angular distribution of $^{11}\text{Be}+d$ system at 295.9 MeV. We investigate twelve different nuclear potentials which consist of Gaussian-Gaussian (G-G), Exponential-Exponential (E-E), Yukawa-Yukawa (Y-Y), Woods Saxon-Woods Saxon (WS-WS), Woods Saxon Squared-Woods Saxon Squared ($\text{WS}^2\text{-WS}^2$), Gaussian-Yukawa (G-Y), Yukawa-Gaussian (Y-G), Gaussian-Woods Saxon (G-WS), Woods Saxon-Gaussian (WS-G), Gaussian-Woods Saxon Squared (G- WS^2), Woods Saxon Squared-Gaussian ($\text{WS}^2\text{-G}$) and Exponential-Gaussian (E-G) potentials. Our results are compared with the literature results as well as the experimental data. Thus, the similarities and differences of the nuclear potentials evaluated with this study are displayed.

Keywords: Nuclear Potential, Optical Model, Elastic Scattering.

Farklı Nükleer Potansiyeller ile $^{11}\text{Be}+d$ Reaksiyonunun İncelenmesi

Öz

Bu çalışmada, 295.9 MeV'de $^{11}\text{Be}+d$ sisteminin elastik saçılma açılma dağılımını açıklamada çeşitli nükleer potansiyellerin etkinliğini görmeği amaçlıyoruz. Gaussian-Gaussian (G-G), Exponential-Exponential (E-E), Yukawa-Yukawa (Y-Y), Woods Saxon-Woods Saxon (WS-WS), Woods Saxon Squared-Woods Saxon Squared ($\text{WS}^2\text{-WS}^2$), Gaussian-Yukawa (G-Y), Yukawa-Gaussian (Y-G), Gaussian-Woods Saxon (G-WS), Woods Saxon-Gaussian (WS-G), Gaussian-Woods Saxon Squared (G- WS^2), Woods Saxon Squared-Gaussian ($\text{WS}^2\text{-G}$) ve Exponential-Gaussian (E-G) potansiyellerinden oluşan on iki farklı nükleer potansiyeli inceliyoruz. Sonuçlarımız deneysel datanın yanı sıra literatür sonuçlarıyla karşılaştırılıyor. Böylece, bu çalışmayla değerlendirilen nükleer potansiyellerin benzerlikleri ve farklılıkları gösteriliyor.

Anahtar kelimeler: Nükleer Potansiyel, Optik Model, Elastik Saçılma.

1. Introduction

The elastic scattering data of $^{11}\text{Be}+d$ reaction at $E_{\text{Lab}} = 295.9$ MeV has been measured for the first time by Chen et al. [1]. They have applied optical potentials and an extended version of the Continuum Discretized Coupled-Channels (XCDCC) formalism in order to analyze the experimental data. Then, four-body continuum effect on $^{11}\text{Be}+d$ scattering has been investigated with a new reaction model, a four-body extension of the Continuum Discretized Coupled Channel (CDCC) model [2]. We think that it is important to examine the effects of phenomenological nuclear potentials on the elastic scattering of $^{11}\text{Be}+d$ reaction.

In this work, we investigate twelve different nuclear potentials which consist of Gaussian-Gaussian (G-G), Exponential-Exponential (E-E), Yukawa-Yukawa (Y-Y), Woods Saxon-Woods Saxon (WS-WS), Woods Saxon Squared-Woods Saxon Squared ($\text{WS}^2\text{-WS}^2$), Gaussian-Yukawa (G-Y), Yukawa-Gaussian (Y-G), Gaussian-Woods Saxon (G-WS), Woods Saxon-Gaussian (WS-G), Gaussian-Woods Saxon Squared (G- WS^2), Woods Saxon Squared-Gaussian ($\text{WS}^2\text{-G}$) and Exponential-Gaussian (E-G) potentials. We compare all the theoretical results with both the literature and the experimental data.

*Sorumlu yazar: maygun@beu.edu.tr

Geliş Tarihi: 10/12/2017 Kabul Tarihi: 19/01/2018

2. Theoretical Formalism

In our work, to see the state of being feasible of different nuclear potentials in obtaining the elastic scattering angular distributions, the optical model is used. In this context, the total potential is assumed as

$$V_{total}(r) = V_N(r) + V_C(r) \quad (1)$$

where V_N is nuclear potential and V_C is Coulomb potential.

2.1. Gaussian-Gaussian (G-G) Potential

Firstly, we assume Gaussian-Gaussian (G-G) potential given by [3,4]

$$V_N^{G-G}(r) = -V_1 \exp\left[-\left(\frac{r-R_{v1}}{a_{v1}}\right)^2\right] - V_2 \exp\left[-\left(\frac{r-R_{v2}}{a_{v2}}\right)^2\right] \quad (2)$$

where $R_i = r_i(A_P^{1/3} + A_T^{1/3})$, $i=v1, v2$, and A_P and A_T are mass numbers of projectile and target nuclei, respectively.

2.2. Exponential-Exponential (E-E) Potential

Secondly, we handle Exponential-Exponential (E-E) potential parametrized by [3,4]

$$V_N^{E-E}(r) = -V_1 \exp\left[-\left(\frac{r-R_{v1}}{a_{v1}}\right)\right] - V_2 \exp\left[-\left(\frac{r-R_{v2}}{a_{v2}}\right)\right]. \quad (3)$$

2.3. Yukawa-Yukawa (Y-Y) Potential

Thirdly, the real and imaginary potentials are considered as Yukawa-Yukawa (Y-Y) potential presented by [3,4]

$$V_N^{Y-Y}(r) = -V_1 \frac{\exp\left[-\left(\frac{r-R_{v1}}{a_{v1}}\right)\right]}{r} - V_2 \frac{\exp\left[-\left(\frac{r-R_{v2}}{a_{v2}}\right)\right]}{r}. \quad (4)$$

2.4. Woods Saxon-Woods Saxon (WS-WS) Potential

Another nuclear potential is Woods Saxon-Woods Saxon (WS-WS) potential shown by [3,4]

$$V_N^{WS-WS}(r) = -\frac{V_1}{1+\exp\left(\frac{r-R_{v1}}{a_{v1}}\right)} - \frac{V_2}{1+\exp\left(\frac{r-R_{v2}}{a_{v2}}\right)}. \quad (5)$$

2.5. Woods Saxon Squared-Woods Saxon Squared (WS²-WS²) Potential

Woods Saxon Squared-Woods Saxon Squared (WS²-WS²) potential is formulated by [3,4]

$$V_N^{WS^2-WS^2}(r) = -\frac{V_1}{\left[1+\exp\left(-\left(\frac{r-R_{v1}}{a_{v1}}\right)\right)\right]^2} - \frac{V_2}{\left[1+\exp\left(-\left(\frac{r-R_{v2}}{a_{v2}}\right)\right)\right]^2}. \quad (6)$$

2.6. Gaussian-Yukawa (G-Y) Potential

Here, Gaussian-Yukawa potential (G-Y) is evaluated as [3,4]

$$V_N^{G-Y}(r) = -V_1 \exp\left[-\left(\frac{r-R_{v1}}{a_{v1}}\right)^2\right] - V_2 \frac{\exp\left[-\left(\frac{r-R_{v2}}{a_{v2}}\right)\right]}{r}. \quad (7)$$

2.7. Yukawa-Gaussian (Y-G) Potential

Yukawa-Gaussian potential (Y-G) is shown by [3]

$$V_N^{Y-G}(r) = -V_1 \frac{\exp\left[-\left(\frac{r-R_{v1}}{a_{v1}}\right)\right]}{r} - V_2 \exp\left[-\left(\frac{r-R_{v2}}{a_{v2}}\right)^2\right]. \quad (8)$$

2.8. Gaussian-Woods Saxon (G-WS) Potential

Gaussian-Woods Saxon (G-WS) potential is taken as [3,4]

$$V_N^{G-WS}(r) = -V_1 \exp\left[-\left(\frac{r-R_{v1}}{a_{v1}}\right)^2\right] - \frac{V_2}{1+\exp\left(\frac{r-R_{v2}}{a_{v2}}\right)}. \quad (9)$$

2.9. Woods Saxon-Gaussian (WS-G) Potential

Woods Saxon-Gaussian (WS-G) nuclear potential is displayed in the following form [3]

$$V_N^{WS-G}(r) = -\frac{V_1}{1+\exp\left(\frac{r-R_{v1}}{a_{v1}}\right)} - V_2 \exp\left[-\left(\frac{r-R_{v2}}{a_{v2}}\right)^2\right]. \quad (10)$$

2.10. Gaussian-Woods Saxon Squared (G-WS²) Potential

Here, Gaussian-Woods Saxon Squared (G-WS²) potential is thought as [3]

$$V_N^{G-WS^2}(r) = -V_1 \exp\left[-\left(\frac{r-R_{v1}}{a_{v1}}\right)^2\right] - \frac{V_2}{\left[1+\exp\left(-\left(\frac{r-R_{v2}}{a_{v2}}\right)\right)\right]^2}. \quad (11)$$

2.11. Woods Saxon Squared-Gaussian (WS²-G) Potential

Another potential is Woods Saxon Squared-Gaussian (WS²-G) potential shown by [3]

$$V_N^{WS^2-G}(r) = -\frac{V_1}{\left[1+\exp\left(-\left(\frac{r-R_{v1}}{a_{v1}}\right)\right)\right]^2} - V_2 \exp\left[-\left(\frac{r-R_{v2}}{a_{v2}}\right)^2\right]. \quad (12)$$

2.12. Exponential-Gaussian (E-G) Potential

Finally, Exponential-Gaussian (E-G) potential is parametrized by [3]

$$V_N^{E-G}(r) = -V_1 \exp\left[-\left(\frac{r-R_{v1}}{a_{v1}}\right)\right] - V_2 \exp\left[-\left(\frac{r-R_{v2}}{a_{v2}}\right)^2\right]. \quad (13)$$

3. Results and Discussion

The elastic scattering angular distributions of $^{11}\text{Be}+d$ reaction at $E_{\text{Lab}}=295.9$ MeV have been obtained by using G-G, E-E, Y-Y, WS-WS, $\text{WS}^2\text{-WS}^2$, G-Y, Y-G, G-WS, WS-G, G- WS^2 , $\text{WS}^2\text{-G}$, and E-G nuclear potentials. Each of the parameters of the nuclear potentials has been listed in Table 1. In addition, the cross sections obtained from the nuclear potential calculations have been given in Table 1.

Table 1. The optical model parameters and cross-sections obtained for G-G, E-E, Y-Y, WS-WS, $\text{WS}^2\text{-WS}^2$, G-Y, Y-G, G-WS, WS-G, G- WS^2 , $\text{WS}^2\text{-G}$, and E-G nuclear potentials of $^{11}\text{Be}+d$ reaction investigated by using the optical model

| Potential | V_1 (MeV) | r_{v1} (fm) | a_{v1} (fm) | V_2 (MeV) | r_{v2} (fm) | a_{v2} (fm) | σ_R (mb) |
|---------------------------|----------------|------------------|------------------|----------------|------------------|------------------|--------------------|
| G-G | 22.8 | 0.849 | 0.588 | 14.0 | 1.402 | 0.51 | 747.9 |
| E-E | 19.0 | 1.20 | 0.60 | 10.0 | 0.950 | 0.50 | 780.9 |
| Y-Y | 12.0 | 0.95 | 0.50 | 16.0 | 1.400 | 0.40 | 686.7 |
| WS-WS | 20.0 | 0.95 | 0.50 | 33.0 | 1.300 | 0.30 | 812.8 |
| $\text{WS}^2\text{-WS}^2$ | 20.0 | 1.00 | 0.50 | 35.0 | 1.400 | 0.45 | 809.3 |
| G-Y | 15.0 | 0.95 | 0.50 | 43.5 | 1.350 | 0.50 | 807.7 |
| Y-G | 10.0 | 1.30 | 0.50 | 24.0 | 1.350 | 0.50 | 812.8 |
| G-WS | 20.0 | 1.05 | 0.50 | 13.0 | 1.195 | 0.50 | 719.5 |
| WS-G | 20.0 | 1.18 | 0.68 | 11.0 | 1.195 | 0.50 | 540.5 |
| G- WS^2 | 17.0 | 1.09 | 0.50 | 13.0 | 1.160 | 0.50 | 505.6 |
| $\text{WS}^2\text{-G}$ | 6.50 | 1.40 | 0.35 | 23.0 | 1.160 | 0.50 | 639.4 |
| E-G | 10.6 | 1.00 | 0.30 | 40.0 | 1.130 | 0.52 | 619.0 |

Figure 1 shows the elastic scattering results obtained from the theoretical calculations of twelve nuclear potentials as compared with the experimental data. In this respect, different situations depending on the structures of the analyzed potentials have been observed. It has been seen that the real part of G-Y potential plays an important role on theoretical results and Y potential is very effective in the calculations compared to G potential. Similar changes to G-Y potential calculations have been observed for Y-Y, WS-WS and $\text{WS}^2\text{-WS}^2$ potential calculations. The changes in the parameters of the imaginary potential have been found to have a significant effect on the theoretical results.

On the other hand, we have observed a different situation in the theoretical calculations of G-G, E-E, G-WS, WS-G, G- WS^2 , $\text{WS}^2\text{-G}$ and Y-G potentials compared to other potential calculations. We have noticed that not only the imaginary potential but also the real potential are very effective on the theoretical calculations. In this context, the variation of real potential parameters have changed significantly the theoretical results. We have observed that the amplitude values for the calculations of Y-G potential are higher than the other potentials. In addition, we have seen that the G-G potential results are much better than the results of other potentials when compared the theoretical results of all the potentials.

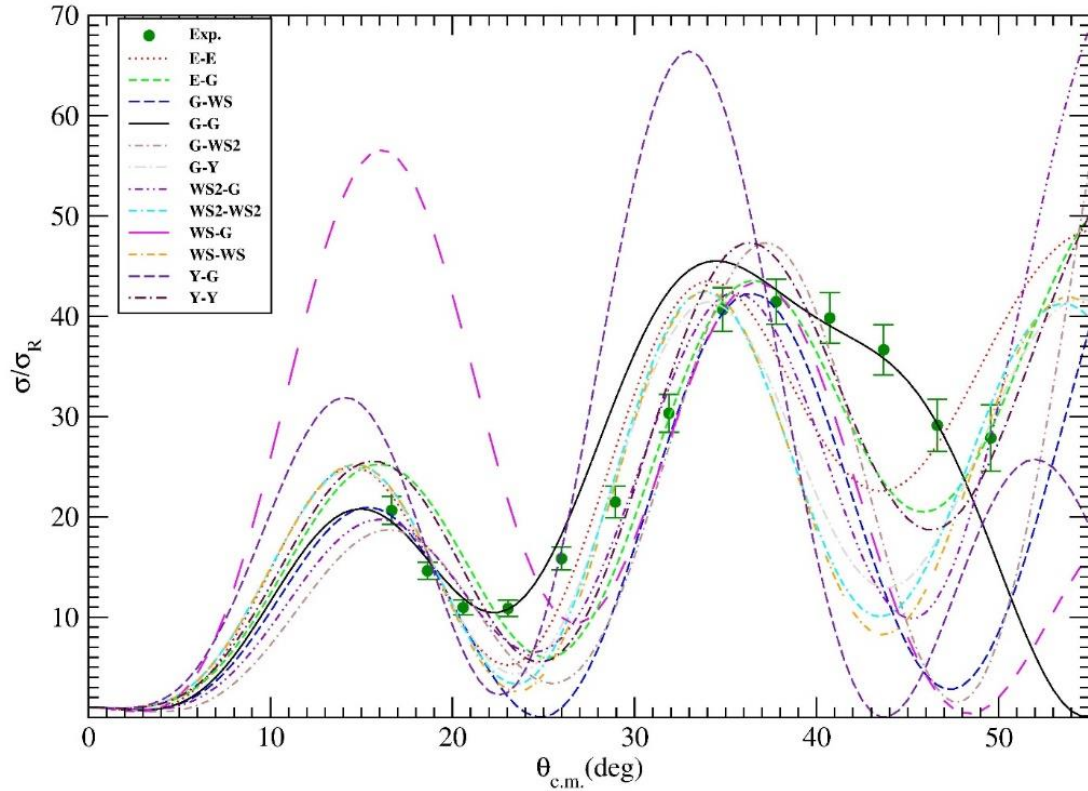


Figure 1. The elastic scattering angular distributions of $^{11}\text{Be}+d$ reaction at $E_{\text{Lab}}=295.9$ MeV by using G-G, E-E, Y-Y, WS-WS, $\text{WS}^2\text{-WS}^2$, G-Y, Y-G, G-WS, WS-G, G-WS^2 , $\text{WS}^2\text{-G}$, and E-G nuclear potentials in comparison with the experimental data. The circles show the experimental data, which have been taken from [1]

Also, we have aimed to make a comparative study in order to see the effectiveness of our work. For this purpose, we have used the results of G-G nuclear potential which have given better results with the experimental data than the other nuclear potentials evaluated in our study. In Fig. 2, we have compared our results with the theoretical results obtained by using optical potentials and the XCDCC formalism by Chen et al. [1]. It can be clearly seen that G-G results obtained with this work are better than the other theoretical results. At small angles, G-G results are in very good agreement with data. Whereas both our results and literature miss the middle angles of the experimental data. On the other hand, at forward angles, our results are in well agreement with the data in comparison with the literature results.

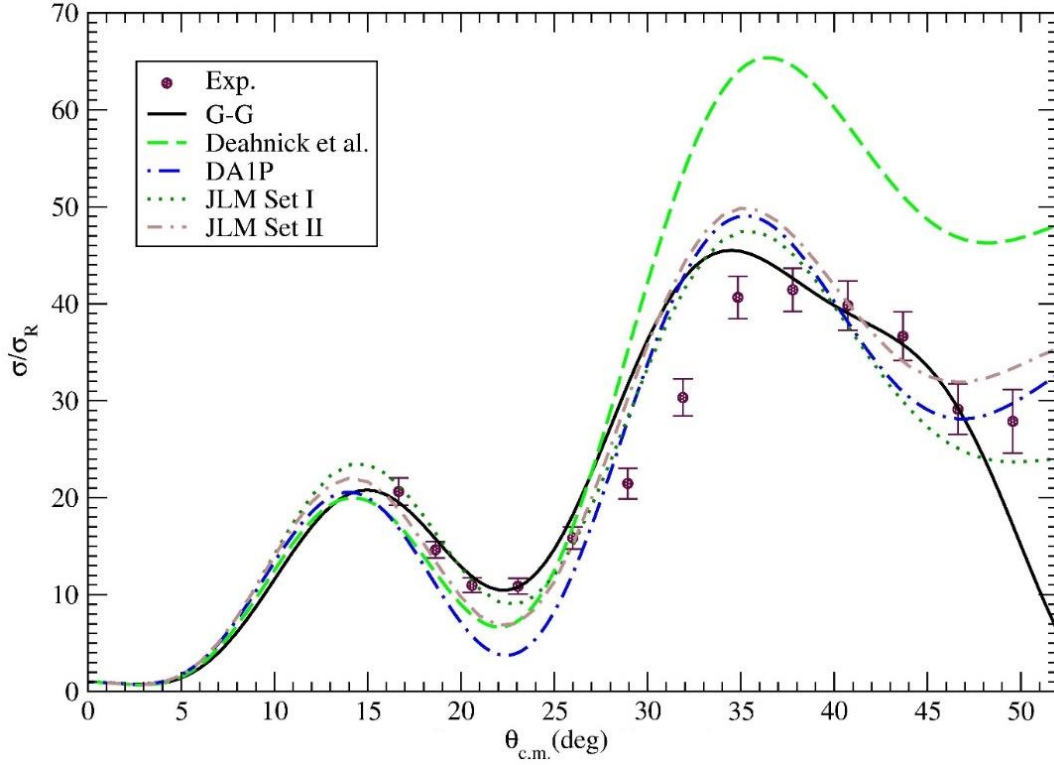


Figure 2. Comparison of G-G and literature results for the elastic scattering angular distribution of $^{11}\text{Be}+d$ reaction at $E_{\text{Lab}}=295.9$ MeV

4. Summary

In the present study, we have examined the effect of nuclear potentials on the elastic scattering data of $^{11}\text{Be}+d$ reaction at $E_{\text{Lab}} = 295.9$ MeV. For this, we have considered twelve different nuclear potentials and have applied in obtaining the elastic cross section of $^{11}\text{Be}+d$ reaction. We have observed that the theoretical results are sensitive to the shapes of the nuclear potentials used in the calculations. We have noticed that G-G potential is in better agreement with the experimental in comparison with the other potentials. Then, we have compared our results with the literature. We have observed that G-G results are better than the literature results.

Acknowledgments

Author would like to thank J. L. Lou for providing the experimental data and the theoretical results.

References

1. Chen J., et al. 2016. Elastic Scattering and Breakup of ^{11}Be on Deuterons at 26.9A MeV, Phys. Rev. C, 94: 064620.
2. Descouvemont P. 2017. Four-body Continuum Effects in $^{11}\text{Be}+d$ Scattering, Phys. Lett. B, 772: 14.
3. Thompson, I.J. 2011. Fresco Version 2.9, <http://www.fresco.org.uk>
4. Aygün, M. 2017. A Theoretical Analysis of Quasi-elastic Scattering of ^7Li by ^{120}Sn using Various Nuclear Potentials, Journal of Nuclear Sciences, 4: 1-6.